Biophysical Chemistry 140 (2009) 9–15

Contents lists available at ScienceDirect

Biophysical Chemistry

journal homepage: http://www.elsevier.com/locate/biophyschem

α-Synuclein aggregation variable temperature and variable pH kinetic data: A re-analysis using the Finke–Watzky 2-step model of nucleation and autocatalytic growth

Aimee M. Morris, Richard G. Finke *

Department of Chemistry, Colorado State University, Fort Collins, CO 80523, United States

ARTICLE INFO

Article history:
Received 8 October 2008
Received in revised form 6 November 2008
Accepted 6 November 2008
Available online 18 November 2008

Keywords:
α-Synuclein aggregation
Variable temperature
Variable pH
Kinetic analysis
F–W model

ABSTRACT

The aggregation of proteins is believed to be intimately connected to many neurodegenerative disorders. We recently reported an "Ockham's razor"/minimalistic approach to analyze the kinetic data of protein aggregation using the Finke–Watzky (F–W) 2-step model of nucleation (A→B, rate constant k_1) and autocatalytic growth (A+B→2B, rate constant k_2). With that kinetic model we have analyzed 41 representative protein aggregation data sets in two recent publications, including amyloid β, α-synuclein, polyglutamine, and prion proteins (Morris, A. M., et al. (2008) Biochemistry 47, 2413-2427; Watzky, M. A., et al. (2008) Biochemistry 47, 10790–10800). Herein we use the F–W model to reanalyze protein aggregation kinetic data obtained under the experimental conditions of variable temperature or pH 2.0 to 8.5. We provide the average nucleation (k_1) and growth (k_2) rate constants and correlations with variable temperature or varying pH for the protein α-synuclein. From the variable temperature data, activation parameters $\Delta G^{\ddagger}$, $\Delta H^{\ddagger}$, and $\Delta S^{\ddagger}$ are provided for nucleation and growth, and those values are compared to the available parameters reported in the previous literature determined using an empirical method. Our activation parameters suggest that nucleation and growth are energetically similar for α-synuclein aggregation ($\Delta G^{\ddagger}_{\text{nucleation}}$=23(3) kcal/mol; $\Delta G^{\ddagger}_{\text{growth}}$=22(1) kcal/mol at 37 °C). From the variable pH data, the F–W analyses show a maximal k_1 value at pH ~3, as well as minimal k_1 near the isoelectric point (pI) of α-synuclein. Since solubility and net charge are minimized at the pI, either or both of these factors may be important in determining the kinetics of the nucleation step. On the other hand, the k_2 values increase with decreasing pH (i.e., do not appear to have a minimum or maximum near the pI) which, when combined with the k_1 vs. pH (and pI) data, suggest that solubility and charge are less important factors for growth, and that charge is important in the k_1, nucleation step of α-synuclein. The chemically well-defined nucleation (k_1) rate constants obtained from the F–W analysis are, as expected, *different than the 1/lag-time empirical constants previously obtained*. However, $k_2 \times [A]_0$ (where k_2 is the rate constant for autocatalytic growth and $[A]_0$ is the initial protein concentration) is related to the empirical constant, k_{app} obtained previously. Overall, the average nucleation and average growth rate constants for α-synuclein aggregation as a function of pH and variable temperature have been quantitated. Those values support the previously suggested formation of a partially folded intermediate that promotes aggregation under high temperature or acidic conditions.

1. Introduction

The processes of nucleation and growth are of central importance to many different neurological disorders since the aggregation of certain proteins is hypothesized in the literature to be intimately linked to the cause of numerous neurodegenerative diseases [1–6]. For instance, the aggregation of α-synuclein has been hypothesized to be the underlying cause of Parkinson's disease [5]. The ability to monitor and detect protein aggregation is, therefore, of importance and may lead to possible therapeutic treatments.

Recently, we reviewed the literature relevant to the mechanism(s) of protein aggregation and found five classes of proposed kinetic mechanisms for the aggregation of proteins [7]. Experimentally, we found that the "Ockham's razor" [8]/minimalistic, Finke–Watzky (F–W) 2-step model, Scheme 1, is able to fit a wide variety of kinetic data and

$$A \xrightarrow{k_1} B$$
$$A + B \xrightarrow{k_2} 2B$$

Scheme 1. The minimalistic, "Ockham's razor" Finke–Watzky (F–W) 2-step kinetic model of nucleation followed by autocatalytic growth [11].

* Corresponding author. 1872 Campus Delivery C213, Fort Collins, CO 80523-1872, United States. Fax: +1 970 491 1801.
E-mail address: rfinke@lamar.colostate.edu (R.G. Finke).

0301-4622/$ – see front matter © 2008 Elsevier B.V. All rights reserved.
doi:10.1016/j.bpc.2008.11.003

provide quantitative rate constants corresponding to the nucleation and growth of protein aggregates [9,10].

The F–W 2-step model was originally developed for transition-metal nanocluster nucleation and growth [11] but has recently been applied to a wider range of natural growth phenomena [12] including, protein aggregation [9,10] kinetics. In protein aggregation, A is the monomeric form of the protein, B is the polymeric form of the protein aggregate, and k_1 and k_2 correspond to the average rate constants for nucleation and growth, respectively, rigorously defined kinetically by the F–W 2-step kinetic model in Scheme 1.

Recently we reported that the F–W model is able to fit the kinetic data in 14 different data sets of protein aggregation relevant to Alzheimer's, Parkinson's, and Huntington's diseases [9], as well as 27 data sets for yeast and mammalian prion aggregation kinetic data [10]. The F–W fits to these protein aggregation data sets yielded the first quantitative rate constants for both nucleation (k_1) and growth (k_2) in these systems [9,10]. Those individual rate constants in turn yielded insights into factors such as the N-terminal portion and Gln/Asn rich regions that affect nucleation more than growth, while other factors such as the C-terminal portion affects growth and not nucleation in model yeast prion systems relevant to prion diseases [10].

Herein we examine α-synuclein (140 amino acids; ~14,000 MW) aggregation variable temperature and variable pH kinetic data from a classic study from A. L. Fink's laboratories[1] using the F–W model. This protein system was previously analyzed using one method available at the time, namely an empirical approach [13] (see the Results and Discussion section, *vide infra*). Specifically, herein we address the following questions: (i) Is there any correlation between the k_1 and k_2 values for nucleation and growth and the empirical constants determined previously, 1/lag-time and k_{app} [13]? (ii) Do the activation parameters obtained from the variable temperature analysis using the F–W model correspond to the activation parameters reported using empirical methods? (iii) What is the correlation between the pH value and the nucleation and growth rate constants obtained from the F–W analysis? (iv) How do any correlations observed and resultant insights compare to those observed from empirical treatments of the variable pH data? (v) Are our kinetic analyses consistent with the prior finding [13] that acidic pH or increased temperature causes the formation of a partially folded intermediate that promotes α-synuclein aggregation? And lastly, (vi) what physical/biochemical insights can we derive from the deconvoluted, well-defined nucleation (k_1) and autocatalytic growth (k_2) rate constants?

2. Experimental

2.1. Selection of data sets for analysis

The data fit in the Results and Discussion section were selected from searches of the literature (using Scifinder Scholar) that displayed variable temperature or variable pH kinetic data for α-synuclein aggregation and also provided the original raw data (i.e., the temperature or pH kinetic curves). The system chosen was Fink and co-workers' scholarly, expert biophysical studies of α-synuclein aggregation [13].

2.2. Data analysis and curve fitting

Data were extracted (digitized) from published kinetic curves using Engauge Digitizer 2.12 and fit by the analytical equation shown in Eq. (1) corresponding to the F–W model (Scheme 1) using Origin 7.0, all as previously described [9]. The resultant rate constants for each data set were then plotted using Excel 11.3.3 and the activation parameters were calculated using the Eyring equation, Eq. ((2), where k is the rate constant, T is temperature, R is the universal gas constant, k_B is Boltzmann's constant, and h is Planck's constant.

$$[B]_t = [A]_0 - \frac{\frac{k_1}{k_2} + [A]_0}{1 + \frac{k_1}{k_2[A]_0}\exp(k_1 + k_2[A]_0)t} \quad (1)$$

$$\ln\frac{k}{T} = \frac{-\Delta H^{\ddagger}}{RT} + \ln\frac{k_b}{h} + \frac{\Delta S^{\ddagger}}{R} \quad (2)$$

3. Results and discussion

3.1. Previous α-synuclein aggregation kinetic data and analysis by an empirical method

Previously α-synuclein aggregation was induced by increasing temperature or decreasing pH and monitoring the aggregation kinetics using ThT fluorescence [13]. The goal of that study [13] was to test the hypothesis that higher temperature or lower pH would induce the natively unfolded α-synuclein into a partially folded, more aggregation prone, intermediate state. After following the kinetics of α-synuclein aggregation and performing other biophysical studies [13] the authors noted, "such [kinetic] curves are consistent with a nucleation-dependent polymerization model" [13].

The variable temperature and pH kinetic data was previously published and analyzed via the empirical equation shown in Eq. (3) where Y is the fluorescence intensity, $(y_i + m_i x)$ is the initial slope of the line during the lag phase, $(y_f + m_f x)$ is the final slope of the line after the growth has ended, and χ_0 is the time to reach 50% maximum fluorescence intensity [13]. From Eq. (3) the empirical constants[2] of $k_{app} = 1/\tau$ and 1/lag-time $= 1/(\chi_0 - 2\tau)$ are calculated [13]. As these equations show, the lag time and k_{app} are both dependent upon $1/\tau$ in the empirical model. While Eq. (3) is able to fit the published kinetic data [13], the authors were careful to note, "This expression is unrelated to the underlying molecular events, but provides a convenient method for comparison of the kinetics of fibrillation" [13].

$$Y = (y_i + m_i x) + \frac{(v_f + m_f x)}{1 + e^{-\left(\frac{X-\chi_0}{\tau}\right)}} \quad (3)$$

It is of interest, therefore, to analyze this α-synuclein aggregation data by the F–W 2-step nucleation and autocatalytic growth model to (i) see if the F–W model will fit the data, and if so (ii) to obtain discrete, chemically well-defined nucleation (k_1) and autocatalytic growth (k_2) rate constants, as well as (iii) to see if our quantitative kinetic results support or refute the original hypothesis [13] of increased temperature or decreased pH causing the formation of a partially folded intermediate.

[1] We were unaware until after we completed this project that Professor A. L. Fink had passed away. We originally picked his laboratory's data set and paper because of the high quality of data and science in that paper; indeed, we had hoped to initiate a collaboration by sending him a copy of this paper and sharing co-authorship with him. We dedicate this paper to Professor Fink's highly productive career and superb science. We wish we'd had the chance to know him personally and collaborate with him and his research group. We thank Professor G. Millhauser as UC Santa Cruz for his help and advice in constructing this dedication to Professor Fink.

[2] The prior work refers to k_{app} as an apparent first order rate constant. However, since k_{app} is not defined in the usual way by a well-defined and balanced chemical reaction, it is not a true rate constant in a rigorous sense. Hence, we have referred to both 1/lag-time and k_{app} as empirical constants throughout the text. This point is not trivial. In fact, a review of the protein aggregation kinetic and modeling literature [7] shows that a failure to connect words, concepts, and their associated rate constants to *balanced chemical reactions* (as is the protocol of rigorous chemical kinetics) has contributed to considerable confusion in the protein aggregation literature [7]. Obviously, Professor Fink and co-workers were aware of this point as the quotation in the text of the original paper indicates ("This expression is unrelated to the underlying molecular events, but provides a convenient method for comparison of the kinetics of fibrillation") [13].

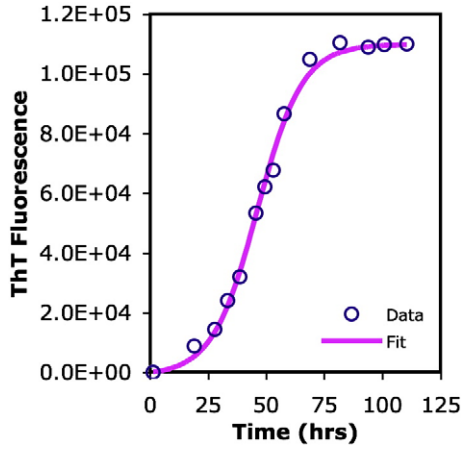

Fig. 1. Literature α-synuclein aggregation at 37 °C kinetic data [13] and the fit by the F–W 2-step model. The resultant rate constants are $k_1 = 8(2)\times10^{-4}$ h^{-1} and $k_2 = 1.5(1)\times10^{-3}$ μM^{-1} h^{-1} with an $R^2 = 0.9957$.

3.2. Analysis of variable temperature α-synuclein aggregation kinetic data with the F–W 2-step model

Variable temperature data of α-synuclein aggregation [13] were analyzed using the F–W 2-step model. The F–W analysis yields the rate constants for nucleation (k_1) and growth (k_2), along with the coefficient of determination (R^2) for each fit.

3.2.1. Sample F–W fit and rate constants obtained

An example of the graphic fit obtained from the F–W analysis of the variable temperature α-synuclein aggregation kinetic data is given in Fig. 1 (all 4 graphical fits of this data are available in Fig. S1 of the Supporting Information). Shown in Table 1 are the nucleation (k_1) and growth (k_2) rate constants obtained from the F–W analysis. Also given in Table 1 are $k_2[A]_0$ values, where $[A]_0$ is the initial concentration of α-synuclein, along with the coefficient of determination (R^2) values for the fits at each temperature. The $R^2 \geq 0.989$ as well as the visually good fits (Figs. 1 and S1 of the Supporting Information) indicate that the F–W model is able to fit the kinetic data well at each temperature. For comparative purposes, the empirical constants[1] previously obtained via Eq. (3) are also provided in Table 1.

As expected, the k_1 and k_2 *rate constants* obtained from the F–W model are different than the *empirical constants*[1] obtained from Eq. (3), Table 1. However, examination of Table 1 reveals that k_{app} from Eq. (3) appears to be proportional to $k_2[A]_0$ obtained by from the F–W model (*vide infra*). From the k_1 and k_2 rate constants, we observe that both nucleation and growth are faster at higher temperatures, as of course expected and as seen with the previous empirical analysis. The increases in k_1 and k_2 are consistent with the previous idea of an increased concentration and/or aggregation rate of a partially folded intermediate at higher temperatures [13].

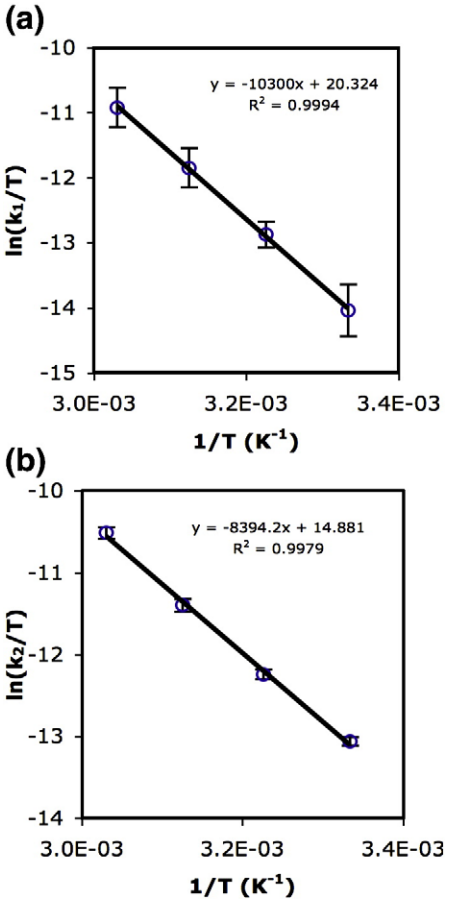

Fig. 2. Eyring plots of (a) k_1 and (b) k_2 for the α-synuclein aggregation system [13]. The error bars were propagated assuming a possibly too large (i.e., upper limit) error in the temperature measurement of ±0.5 °C and since no temperature measurement error bars were given in the original work.

3.2.2. Activation parameter determination

From the Eyring plots shown in Figs. 2a and b, the activation parameters $\Delta G^{\ddagger}$, $\Delta H^{\ddagger}$, and $\Delta S^{\ddagger}$ were obtained for both the nucleation (k_1) and growth (k_2) steps of the α-synuclein aggregation system, Table 2. The activation parameters obtained for the k_1 nucleation and k_2 growth steps are quite similar, a finding that has also been observed in actin aggregation [14]. That said, the importance of $\Delta H^{\ddagger}_{nucleation}$, $\Delta H^{\ddagger}_{growth}$, $\Delta S^{\ddagger}_{nucleation}$, and $\Delta S^{\ddagger}_{growth}$ obtained from the F–W model,

Table 1
The average rate constants and R^2 values obtained from fitting the variable temperature α-synuclein aggregation data [13] with the F–W 2-step model along with comparisons to the empirical constants reported [13] using Eq. (3)

		27 °C	37 °C	47 °C	57 °C
For the F–W analysis:	k_1^a (h^{-1})	$2.4(8)\times10^{-4}$	$8(2)\times10^{-4}$	$2.3(7)\times10^{-3}$	$6(2)\times10^{-3}$
	k_2^a (μM^{-1} h^{-1})	$6.4(4)\times10^{-4}$	$1.5(1)\times10^{-3}$	$3.6(3)\times10^{-3}$	$9.0(7)\times10^{-3}$
	$k_2[A]_0$ (h^{-1})	$4.5(3)\times10^{-2}$	$1.05(7)\times10^{-1}$	$2.5(2)\times10^{-1}$	$6.3(5)\times10^{-1}$
	$R^{2\,b}$	0.9891	0.9957	0.9921	0.9914
From the previous analysis [13]:	1/lag-time ^{c,d} (h^{-1})	4.1×10^{-2}	9.2×10^{-2}	2.5×10^{-1}	6.1×10^{-1}
	k_{app} ^{c,d} (h^{-1})	1.4×10^{-2}	3.4×10^{-2}	1.1×10^{-1}	2.8×10^{-1}

[a]The error bars for k_1 and k_2 are determined by the square root of the reduced χ^2 based on a modified Levenberg–Marquardt algorithm [25].
[b]R^2 is the coefficient of determination and is the square of the correlation coefficient (r). The closer this value is to 1.0, the more precise the analysis is to fitting the data.
[c]The 1/lag-time and k_{app} values were found by digitizing a ln(1/lag-time) and ln(k_{app}) vs. 1/T plot from the original reference [13].
[d] While digitizing the data it became apparent that in order to correspond with the raw variable temperature kinetic data the ln(1/lag-time) and k_{app} vs. 1/T graphs had to be in units of reciprocal seconds. The 1/lag-time and k_{app} were converted to units of h^{-1} for comparison purposes to the analyses presented herein.

Table 2
Activation parameters calculated for α-synuclein aggregation from the Eyring plots shown in Fig. 2 using the F–W analysis and comparison to the empirical parameters previously obtained in the literature

		$\Delta G^{\ddagger}$ (kcal/mol @ 37 °C)	$\Delta H^{\ddagger}$ (kcal/mol)	$\Delta S^{\ddagger}$ (cal/mol K)
From the F–W analysis:	Nucleation, k_1[a]	23(3)	20(3)	−10(10)
	Growth, k_2[a]	22(1)	17(1)	−18(3)
			$\Delta H^{\ddagger}_{emp1}$[b] (kcal/mol)	
From the literature empirical analysis (13)[c,d]:	1/lag-time		17.3(8)[e][27][f]	NA[g]
	k_{app}		19.5(8)[e][27][f]	NA[g]

[a] The error bars are calculated by propagating the error through the Eyring equation using the following equations from Girolami and co-workers [26]:

$$\left(\sigma\Delta H^{\ddagger}\right)^2 = \frac{R^2T_{max}^2T_{min}^2}{(T_{max}-T_{min})^2}\left\{\left(\frac{\sigma T}{T}\right)^2\left[\left(1+T_{min}\frac{\Delta L}{(T_{max}-T_{min})}\right)^2+\left(1+T_{max}\frac{\Delta L}{(T_{max}-T_{min})}\right)^2\right]+2\left(\frac{\sigma k}{k}\right)^2\right\} \text{and}$$

$$\left(\sigma\Delta S^{\ddagger}\right)^2 = \frac{R^2}{(T_{max}-T_{min})^2}\left\{\left(\frac{\sigma T}{T}\right)^2\left[T_{max}^2\left(1+T_{min}\frac{\Delta L}{T_{max}-T_{min}}\right)^2+T_{min}^2\left(1+T_{max}\frac{\Delta L}{T_{max}-T_{min}}\right)^2\right]+\left(\frac{\sigma k}{k}\right)^2\left(T_{max}^2+T_{min}^2\right)\right\}, \text{ where}$$

$\Delta L = [1n(k_{max}/T_{max}) - 1n(k_{min}/T_{min})]$. For σk, we used the largest error bars in the k_1 or k_2 that was observed and assumed an error of 0.5 K for σT. Alternatively, we calculated error bars based on the errors at the 95% (2σ) confidence level for the slope and intercept obtained from the linear regression analysis. However, those resultant error bars are much smaller (by ca. 2–10 fold in $\Delta H^{\ddagger}$ and 3–30 fold in $\Delta S^{\ddagger}$). Therefore, we have reported the larger error bars herein.

[b] We denote the enthalpy of activation from the previous analysis as $\Delta H^{\ddagger}_{emp1}$ since it is derived from empirical constants[1] and is therefore, not a true $\Delta H^{\ddagger}$ value in the unambiguous chemical mechanism sense.

[c] In the literature, Eq. (3) is used to calculate the empirical constants[1] of $k_{app} = 1/\tau$ and 1/lag-time = $1/(\chi_0 - 2\tau)$ [13].

[d] α-Synuclein aggregation was measured from 27 °C to 57 °C; a 30 °C temperature range.

[e] These values were converted from the reported E_a by the following equation: $E_a = \Delta H^{\ddagger} + mRT_{mean}$, where m is the molecularity (taken as 1 in the present case), and T_{mean} is the mean temperature range over which measurements were taken [27].

[f] The error bars reported come from the original analysis [13] and are calculated from the error in the slope of the linear regression fits of the Arrhenius plots.

[g] NA = not available.

and shown in Table 2, is that they refer to the well-defined chemical steps of nucleation and growth, respectively. Application of the F–W model also gives previously unavailable $\Delta S^{\ddagger}$ values.

The activation parameters for α-synuclein aggregation are of interest and merit comment. The values of $\Delta H^{\ddagger}$ for nucleation and growth are both positive for α-synuclein ($\Delta H^{\ddagger}_{nucleation} = 20(3)$ kcal/mol; $\Delta H^{\ddagger}_{growth} = 17(1)$ kcal/mol), while the $\Delta S^{\ddagger}$ for nucleation and growth are compensatingly more negative (i.e., compensationally less favorable) ($\Delta S^{\ddagger}_{nucleation} = -10(10)$ e.u.; $\Delta S^{\ddagger}_{growth} = -18(3)$ e.u.). The enthalpy vs. entropy compensation might be real or might be artifactual [15] due to the moderate temperature range (30 °C) examined; large temperature ranges are known to be required to accurately deconvolute $\Delta G^{\ddagger}$ into $\Delta H^{\ddagger}$ and $\Delta S^{\ddagger}$ [16].

Examination of Table 2 shows that the activation parameter determination using the F–W model yields values that are the same within experimental error as Eq. (3) for $\Delta H^{\ddagger}$. Both the previous [13] and present results are consistent with the idea that $\Delta H^{\ddagger}$ for nucleation and growth are relatively similar.

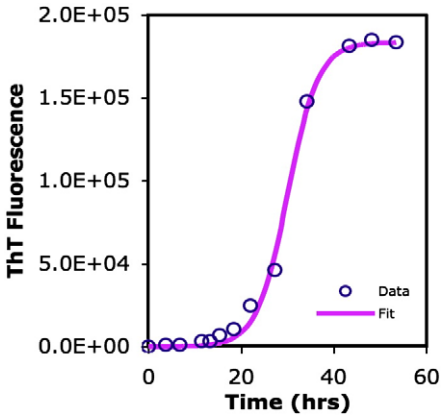

Fig. 3. Literature α-synuclein aggregation kinetic data at pH 5.82 [13] and the fit using the F–W model. Resultant rate constants (and coefficient of determination): $k_1 = 4(2)\times10^{-5}$ h^{-1}; $k_2 = 4.2(3)\times10^{-3}$ μM^{-1} h^{-1} ($R^2 = 0.9965$).

3.3. Analysis of variable pH α-synuclein aggregation kinetic data with the F–W 2-step model

The second aggregation variable examined herein is pH. Interestingly, it has been hypothesized in the literature that a pathological decrease in pH occurs in neurons affected by neurodegenerative diseases resulting in apoptosis [17]. It has also been suggested that lowering the pH causes a reduction in the overall net charge of proteins and thereby increases the aggregation propensity [13]. While selectively maintaining in vivo affected cells at a slightly alkaline pH has been suggested as a possible therapeutic strategy for the treatment of neurodegenerative disorders [17], it is probably not a viable treatment option. However, studying variable pH in vitro may give insights into in vivo factors that could increase the aggregation propensity and intermediate formation of α-synuclein.

Hence, we have reanalyzed the α-synuclein variable pH kinetic data that was previously analyzed using Eq. (3) to give empirical constants[1] 1/lag-time and k_{app} [13]. Fig. 3 shows a representative fit and Fig. S2 of the Supporting Information shows the graphical fits to each of the five pH values examined using the F–W 2-step model. Table 3 shows the *rate* constants obtained from the F–W analyses along with the associated R^2 values. The rate constants obtained by the analytic equation for the 2-

Table 3
The resulting rate constants and R^2 values from the published [13] α-synuclein variable pH data fit by the F–W 2-step model and comparison to the empirical constants reported previously

	pH 1.92	pH 2.79	pH 4.08	pH 5.82	pH 7.23/8.52[a]
k_1 (h^{-1})	$3(2)\times10^{-3}$	$1.2(4)\times10^{-2}$	$6(2)\times10^{-5}$	$4(2)\times10^{-5}$	$3.5(6)\times10^{-4}$
k_2 ($\mu M^{-1}h^{-1}$)	$1.3(3)\times10^{-2}$	$1.0(1)\times10^{-2}$	$1.17(5)\times10^{-2}$	$4.2(3)\times10^{-3}$	$1.7(1)\times10^{-3}$
$k_2[A]_0$ (h^{-1})	$9(2)\times10^{-1}$	$7.0(7)\times10^{-1}$	$8.2(3)\times10^{-1}$	$2.9(2)\times10^{-1}$	$1.19(7)\times10^{-1}$
R^2	0.9898	0.9902	0.9993	0.9965	0.9984
1/lag-time (h^{-1})[b]	2.5×10^{-1}	4.4×10^{-1}	1.1×10^{-1}	4.2×10^{-2}	3.5×10^{-2}/ 3.3×10^{-2}
k_{app} (h^{-1})[b]	8.2×10^{-1}	1.0	7.0×10^{-1}	3.4×10^{-1}	1.1×10^{-1}/ 8.6×10^{-2}

[a] While digitizing this data set we were unable to discern between the data points for pH 7.23 and pH 8.52.

[b] These values were obtained by digitizing the pH vs. 1/lag-time and pH vs. k_{app} graphs from the original reference [13].

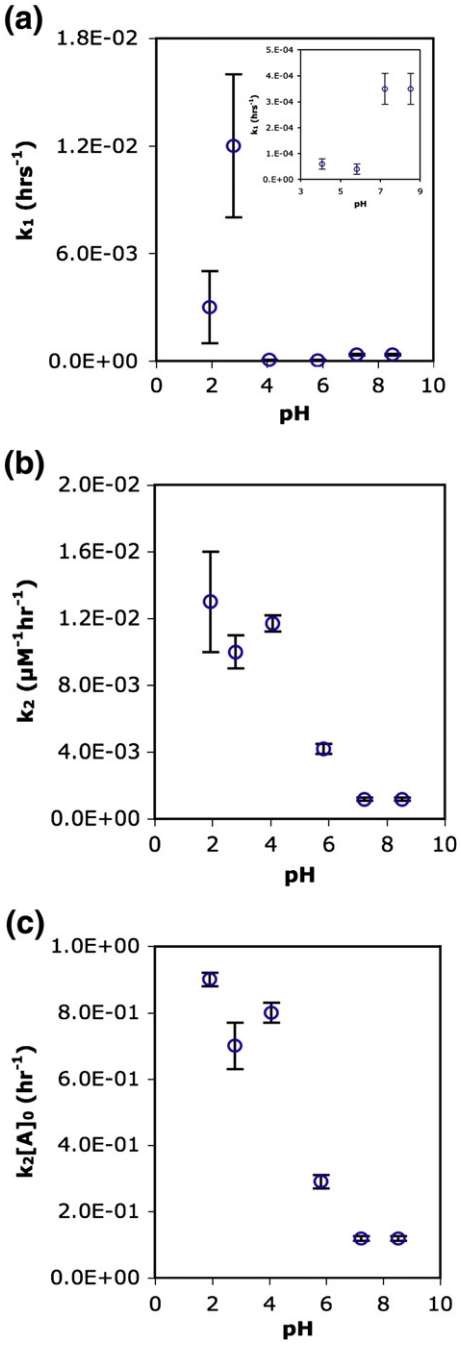

Fig. 4. The (a) k_1, (b) k_2 and (c) $k_2[A]_0$ correlations determined using the F–W 2-step model to varying pH values.

step model (Eq. (1)) are one to two orders of magnitude different than the empirical constants obtained with Eq. (3), Table 3.

3.3.1. Correlations between pH values and nucleation and growth rate constants obtained from the F–W analysis

The correlations obtained using the F–W model for the varying pH data are shown in Fig. 4. Fig. 4a reveals that the k_1 rate constant is increased at pH ~2 and increased by another order of magnitude at pH ~3. From pH ~3 to ~4 the nucleation rate constant is decreased by 3 orders of magnitude. The *slowest* nucleation rate constants occur from pH 4–6 which coincide well with the isoelectric point (pI) of 4.0–4.7 given for α-synuclein [13,18,19]. The k_1 rate constant also increases by an order of magnitude but now from pH ~6 to pH ~7. The data suggest that there is an optimum pH of ca. 3 at which the nucleation rate is greatly enhanced. The result of an optimum pH ~3 is consistent with the previous structural analyses by Fourier transform infrared spectroscopy and small angle X-ray scattering, suggesting that the partially folded intermediate forms between pH 7.5 and 3.0. This optimum pH ~3 is also consistent with the previous CD and ANS fluorescence results which suggest partially folded intermediate formation between pH 5.5 and 3.0 [13]. Assuming that the ThT fluorescence is providing an accurate measure of α-synuclein aggregation, our kinetic analysis suggests that the pH range in which the partially folded intermediate is formed and nucleation is most increased is pH ~3. The minimum nucleation rate constants near the pI also suggest that solubility or net charge (or both) may be important factors in determining the nucleation rate constant for α-synuclein aggregation [20].

The previous kinetic analysis performed via Eq. (3) yielded a correlation of shorter lag-times with decreasing pH values but also revealed the shortest lag-time occurred at pH ~3 [13]. However, over the range of pH measured, the lag-time only changed by one order of magnitude. Our results herein, as well as studies in progress [21], *suggests that the lag-time in sigmoidal protein aggregation curves is not a generally reliable measure of the nucleation rate constant*.

Fig. 4b shows the correlation of increasing k_2 values (i.e., faster growth) with decreasing pH. As expected since the concentration of the protein remains constant, the same correlation holds true for increasing $k_2[A]_0$ with decreasing pH, Fig. 4c. This is also the same correlation previously observed for k_{app} [13]. Hence, it appears that the solubility and charge minima at the pI are not major factors in determining the *growth* rate constants of α-synuclein. More importantly, k_2 should have decreased, not increased, near the pI as did k_1 if decreased solubility of α-synuclein near the pI was the controlling variable. Hence, the combined pH/pI effects on k_2 and k_1 suggest that *charge* is the important variable in determining the α-synuclein nucleation rate constant, k_1.

In short, from the F–W reanalysis of the variable pH data, we confirm the previous findings [13] that: (i) the nucleation rate constant (k_1) is larger at lower pH values and (ii) k_{app}, $k_2[A]_0$, and k_2 increases with decreasing pH values. This supports the previous claim that the nucleation and growth rate constants are increased under acidic conditions [13]. We have, however, added the insights that: (i) the k_1 rate constant seems to be maximal at pH 3 and minimal near the pI, (ii) k_2 increases with pH and does not correlate with the pI, so that (iii) *net charge* is implicated as an important factor in determining

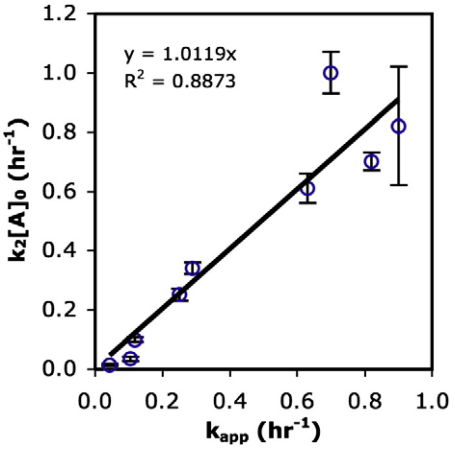

Fig. 5. The k_{app} values obtained from Eq. (3) for both the variable temperature and variable pH data compared to the $k_2[A]_0$ values obtained from the same data but using the F–W 2-step model. The k_{app} and $k_2[A]_0$ values can also be found in Tables 1 and 3.

the k_1 value. In addition, (iv) *the lag-time (i.e., 1/lag-time) is not a generally reliable measure of* k_1.

3.4. Analysis of any relationships of the rate constants obtained from the F–W reanalysis to the empirical constants from Eq. (3)

Fig. 5, as well as examination of Tables 1 and 3, show that the $k_2[A]_0$ values from the F–W model are proportional to the k_{app} values obtained from Eq. (3), (a plot of k_2 vs. k_{app} is also available in the Supporting Information). The $k_2[A]_0 \propto k_{app}$ reflects the fact that both k_{app} and k_2 are proportional to the slope of the growth line [11,13]. In addition, $k_2[A]_0 \propto k_{app}$ is a useful finding that helps add validity to the interpretation from the previously obtained k_{app} [13].

We also attempted to look for any correlations between the empirical constant 1/lag-time and k_1, k_2 (or some combination of k_1 and k_2) from the F–W model. We did not find any apparent correlation (the interested reader is referred to Figs. S3, S4 the Supporting Information to see the plots of k_1, k_1+k_2, $k_1\times k_2$, k_1/k_2, $k_1+k_2[A]_0$, $k_1\times k_2[A]_0$, and $k_1/k_2[A]_0$ vs. 1/lag-time). This again suggests that lag-time is not be an accurate measure of the nucleation rate constant. We were also unable to find any simple mathematical equivalence correlation between Eq. (1) from the F–W model and the empirical Eq. (3) (Scheme S1 of the Supporting Information).

3.5. Caveats and limitations of the F–W kinetic model

The weaknesses of the F–W model, which derive ultimately from its over-simplified nature, have been presented in three other publications for the interested reader [7,9,10]. Briefly, the main limitations are: (i) k_1 and k_2 are averages (although to the extent nucleation tends towards the limit of a simple misfolded protein [21], k_1 should tend towards the limit of the rate constant for that individual step); (ii) B is also an average, so that (iii) important changes in k_1, k_2, or B as a function of aggregation fibril size are hidden. In addition, (iv) other processes such as fibril fragmentation are not treated explicitly [10]. The main advantage of the F–W 2-step model is, however, its ability to deconvolute the average nucleation rate constant, k_1, from the average autocatalytic growth rate constant, k_2, in a model that has rate constants and associated concepts (words; specifically nucleation and autocatalytic growth) rigorously defined by balanced chemical reactions in the normal way of rigorous kinetic and mechanistic science.

4. Conclusions

The contributions from this article are the following:

- The F–W model 2-step has been used to analyze α-synuclein aggregation kinetics under variable temperature and variable pH conditions. Quantitative rate constants with well-defined physical meaning corresponding to both nucleation and growth, k_1 and k_2 respectively, were obtained.
- The k_1 rate constant found using the F–W model differs from the empirical 1/lag-time constant obtained previously. Other, in progress work confirms that 1/lag-time is not a reliable predictor of k_1 [22]. However, $k_2[A]_0$ from the F–W model is proportional to k_{app} from the Eq. (3) empirical treatment, thereby adding validity to the prior determination and interpretation of k_{app}.
- The activation parameter determination for α-synuclein performed herein is the first to our knowledge to report values for $\Delta G^{\ddagger}$, $\Delta H^{\ddagger}$, and $\Delta S^{\ddagger}$ for well-defined nucleation and autocatalytic growth.
- The $\Delta H^{\ddagger}$, $\Delta S^{\ddagger}$, and $\Delta G^{\ddagger}$ of nucleation and growth were found to be approximately equivalent for α-synuclein under the experimental conditions examined.
- The α-synuclein variable pH data analysis shows that the nucleation rate constant, k_1, has a maximal rate constant at pH ~3, as well as minimal rate constant at pH ~4–6. These results are consistent with the previous analysis [13] and further suggests that there is an optimal pH for the nucleation rate constant.
- The growth rate constant, k_2, (as well as $k_2[A]_0$) appears to increase with decreasing pH — that is, the average growth rate constant is faster at lower pH values in the case examined herein. This observation is again consistent with the previous analysis [13]. Furthermore, the k_2 rate constants do not correlate with the pI.
- The combined k_1 and k_2 vs. pH data near the pI of α-synuclein in turn suggest that *net charge* is an important variable in α-synuclein nucleation.
- Overall, our reanalysis quantitates the average nucleation and average growth rate constants and kinetically supports Fink and co-workers' hypothesis [13] of the formation of a partially folded intermediate species that promotes aggregation at higher temperatures or lower pH.
- Other variables that have been hypothesized to either accelerate (e.g., O_2, H_2O_2, or $O_2^{\bullet}$ [23]), or inhibit (e.g., β- or γ-synuclein [24]), α-synuclein aggregation in vivo are of interest for deconvolution into k_1 and k_2 effects by the methods detailed herein.

Finally, it is especially important to acknowledge the original work and contributions of the Professor A. L. Fink and his co-workers [13]. It is their original efforts and α-synuclein kinetic data that have allowed the work and analysis herein to be reported. We are pleased to dedicate this work to Professor Fink's memory.[1]

Acknowledgement

Partial support from NSF grant # 0611588 is gratefully acknowledged.

Appendix A. Supplementary data

Supplementary data associated with this article can be found, in the online version, at doi:10.1016/j.bpc.2008.11.003.

References

[1] M.B. Pepsys, Amyloidosis, Annu. Rev. Med. 57 (2006) 223–241.
[2] F. Chiti, C.M. Dobson, Protein misfolding, functional amyloid, and human disease, Annu. Rev. Biochem. 75 (2006) 333–366.
[3] K. Blennow, M.J. de Leon, H. Zetterberg, Alzheimer's disease, Lancet 368 (2006) 387–403.
[4] G.P. Bates, C. Benn, Huntington's Disease, in: G.P. Bates, P.S. Harper, L. Jones (Eds.), The polyglutamine diseases, Oxford University Press, Oxford, 2002, pp. 429–472.
[5] W. Dauer, S. Przedborski, Parkinson's disease: mechanisms and models, Neuron 39 (2003) 889–909.
[6] S.B. Prusiner, Molecular biology of prion diseases, Science 252 (1991) 1515–1522.
[7] A.M. Morris, M.A. Watzky, and R.G. Finke, Protein aggregation kinetics, mechanism and curve-fitting: a review of the literature, Biochim. Biophys. Acta (in press).
[8] William of Ockham, 1285–1349, as cited by E.A. Moody in: The Encyclopedia of Philosophy, vol 7 (MacMillan, New York, 1967).
[9] A.M. Morris, M.A. Watzky, J.N. Agar, R.G. Finke, Fitting neurological protein aggregation kinetic data via a 2-step, minimal/"Ockham's razor" model: the Finke–Watzky mechanism of nucleation followed by autocatalytic surface growth, Biochemistry 47 (2008) 2413–2427.
[10] M.A. Watzky, A.M. Morris, E.D. Ross, R.G. Finke, Fitting yeast and mammalian prion aggregation kinetic data with the Finke–Watzky two-step model of nucleation and autocatalytic growth, Biochemistry 47 (2008) 10790–10800.
[11] M.A. Watzky, R.G. Finke, Transition metal nanocluster formation kinetic and mechanistic studies. A new mechanism when hydrogen is the reductant: slow, continuous nucleation and fast autocatalytic surface growth, J. Am. Chem. Soc. 119 (1997) 10382–10400.
[12] S.E. Smith, J.M. Sasaki, R.G. Bergman, J.E. Mondloch, R.G. Finke, Platinum-catalyzed phenyl and methyl group transfer from tin to iridium: evidence for an autocatalytic reaction pathway with an unusual preference for methyl transfer, J. Am. Chem. Soc. 130 (2008) 1839–1841.
[13] V.N. Uversky, J. Li, A.L. Fink, Evidence for a partially folded intermediate in α-synuclein fibril formation, J. Biol. Chem. 276 (2001) 10737–10744.
[14] F. Oosawa, S. Asakura, Thermodynamics of the Polymerization of Protein, Academic Press, New York, 1975.
[15] S.W. Benson, Thermochemical Kinetics, 2nd Ed., Wiley, New York, 1976, pp. 21–23.
[16] J. Halpern, Compensation effects in the activation parameters for the homolytic dissociation of transition metal-alkyl bonds, Bull. Chem. Soc. Jpn. 61 (1988) 13–15.

[17] S. Harguindey, S.J. Reshkin, G. Orive, J.L. Arranz, E. Anitua, Growth and trophic factors, pH and the Na+/H+ exchanger in Alzheimer's disease, other neurodegenerative diseases and cancer: new therapeutic possibilities and potential dangers, Curr. Alzheimer Res. 4 (2007) 53–65.
[18] V.N. Uversky, J.R. Gillespie, A.L. Fink, Why are "natively unfolded" proteins unstructured under physiologic conditions? Proteins Struct. Funct. Genet. 41 (2000) 415–427.
[19] R. Sharon, I. Bar-Joseph, M.P. Frosch, D.M. Walsh, J.A. Hamilton, D.J. Selkoe, The formation of highly soluble oligomers of α-synuclein is regulated by fatty acids and enhanced in Parkinson's disease, Neuron 37 (2003) 583–595.
[20] D. Voet, J.G. Voet, Biochemistry, 3rd Ed., Wiley, New York, 2004, pp. 131–133.
[21] S. Chen, F.A. Ferrone, R. Wetzel, Huntington's disease age-of-onset linked to polyglutamine aggregation nucleation, Proc. Natl. Acad. Sci. USA 99 (2002) 11884–11889.
[22] A.M. Morris, E.D. Ross, and R.G. Finke, studies in progress.
[23] M.E. Götz, K. Double, M. Gerlach, M.B.H. Youdim, P. Riederer, The relevance of iron in the pathogenesis of Parkinson's disease, Ann. N. Y. Acad. Sci. 1012 (2004) 193–208.
[24] A.L. Fink, The aggregation and fibrillation of α-synuclein, Acc. Chem. Res. 39 (2006) 628–634.
[25] W.H. Press, B.P. Flannery, S.A. Teukolsky, W.T. Vetterling, Numerical Recipes, Cambridge University, Cambridge, 1989.
[26] P.M. Morse, M.D. Spencer, S.R. Wilson, G.S. Girolami, A static agostic α-CH•••M interaction observable by NMR spectroscopy: synthesis of the chromium(II) alkyl $[Cr_2(CH_2SiMe_3)_6]^{2-}$ and its conversion to the unusual "windowpane" bis(metallacycle) complex $[Cr(\kappa 2\text{-}C,C'\text{-}CH_2SiMe_2CH_2)_2]^{2-}$, Organometallics 13 (1994) 1646–1655.
[27] D.M. Golden, Standard states for thermochemical and activation parameters, J. Chem. Educ. 48 (1971) 235–237.